

**Protein Structure and Folding:
Molecular Determinants of Matrix
Metalloproteinase-12 Covalent
Modification by a Photoaffinity Probe:
INSIGHTS INTO ACTIVITY-BASED
PROBE DEVELOPMENT AND
CONFORMATIONAL VARIABILITY OF
MATRIX METALLOPROTEINASES**



Anne-Sophie Dabert-Gay, Bertrand Czarny,
Laurent Devel, Fabrice Beau, Evelyne
Lajeunesse, Sarah Bregant, Robert Thai,
Athanasios Yiotakis and Vincent Dive
J. Biol. Chem. 2008, 283:31058-31067.
doi: 10.1074/jbc.M805795200 originally published online September 5, 2008

Access the most updated version of this article at doi: [10.1074/jbc.M805795200](https://doi.org/10.1074/jbc.M805795200)

Find articles, minireviews, Reflections and Classics on similar topics on the [JBC Affinity Sites](#).

Alerts:

- [When this article is cited](#)
- [When a correction for this article is posted](#)

[Click here](#) to choose from all of JBC's e-mail alerts

This article cites 42 references, 12 of which can be accessed free at
<http://www.jbc.org/content/283/45/31058.full.html#ref-list-1>

Molecular Determinants of Matrix Metalloproteinase-12 Covalent Modification by a Photoaffinity Probe

INSIGHTS INTO ACTIVITY-BASED PROBE DEVELOPMENT AND CONFORMATIONAL VARIABILITY OF MATRIX METALLOPROTEINASES*

Received for publication, July 29, 2008, and in revised form, September 2, 2008. Published, JBC Papers in Press, September 5, 2008, DOI 10.1074/jbc.M805795200

Anne-Sophie Dabert-Gay[‡], Bertrand Czarny[‡], Laurent Devel[‡], Fabrice Beau[‡], Evelyne Lajeunesse[‡], Sarah Bregant[‡], Robert Thai[‡], Athanasios Yiotakis[§], and Vincent Dive^{‡1}

From the [‡]CEA, Service d'Ingénierie Moléculaire de Protéines, 152, CE-Saclay, Gif/Yvette 91191, Cedex, France and [§]Laboratory of Organic Chemistry, Department of Organic Chemistry, University of Athens, Panepistimiopolis, Zografou, Athens 15771, Greece

Mass spectroscopy, microsequencing, and site-directed mutagenesis studies have been performed to identify in human matrix metalloelastase (hMMP-12) residues covalently modified by a photoaffinity probe, previously shown to be able to covalently label specifically the active site of matrix metalloproteinases (MMPs). Results obtained led us to conclude that photoactivation of this probe in complex with hMMP-12 affects a single residue in human MMP-12, Lys²⁴¹, through covalent modification of its side chain ϵ NH₂ group. Because x-ray and NMR studies of hMMP-12 indicate that Lys²⁴¹ side chain is highly flexible, our data reveal the existence of particular Lys²⁴¹ side-chain conformation in which the ϵ NH₂ group points toward the photolabile group of the probe, an event explaining the high levels of cross-linking yield between hMMP-12 and the probe. Lys²⁴¹ is not conserved in MMPs, thus differences in cross-linking yields observed with this probe between MMP members may be linked to the residue variability observed at position 241 in this family.

Matrix metalloproteinases (MMPs)² belong to a family of structurally related extracellular/cell surface-anchored zinc endoproteinases able to collectively cleave the protein component of the extracellular matrix (1, 2). MMPs are considered to be critical mediators of both normal and pathological tissue remodeling processes (3). MMPs form a group of 23 proteins in humans containing a catalytic domain belonging to the metzincin superfamily (4–8). Their overexpression observed in and associated with various diseases (9), including cancer, arthritis, atherosclerosis, and multiple sclerosis, has stimulated impres-

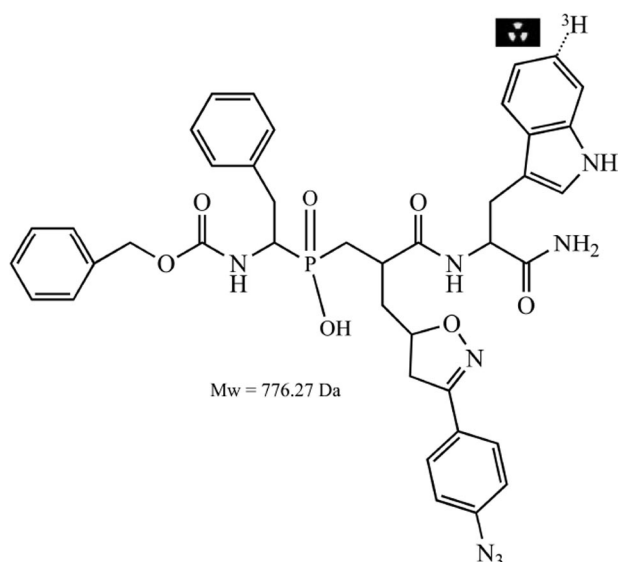
sive effort over the past 20 years to develop synthetic inhibitors able to block potently the uncontrolled activity of these potential therapeutic targets (10, 11). Extremely potent inhibitors of MMPs have been developed, but with the exception of MMP-2 (12), MMP-13 (13, 14), and MMP-12 (15), most of these inhibitors act as broad-spectrum inhibitors of MMPs. Clinical trials based on the use of these broad-spectrum inhibitors in patients with advanced cancers have failed to reach their end points, with severe side effects observed (16). Some reasons for this failure, as discussed in recent studies, suggest that some MMP members promote tumor progression, but others provide a protective effect in different stages of cancer progression (17). This highlights the need to use in clinical setting highly selective inhibitors able to target only the MMPs responsible for tumor progression (18–21). Similar trends have been observed in atherosclerosis, in which some MMP members have opposite effects on plaque stability. In this pathology, MMP-12 has been reported to promote both lesion and plaque extension (22), justifying our current efforts in developing selective MMP-12 inhibitors (15). To further progress on our understanding of the complex roles played by MMPs, probes able to detect and identify which MMPs are expressed under active forms in a complex biological environment have recently been developed (23–26). To be informative, such activity-based probes (ABPs) should covalently and exclusively modify the free form of the protease active site, but not the pro-form or the active form in complex with natural TIMP inhibitors. ABPs for serine and cysteine proteinases have been successfully developed by exploiting the presence of highly conserved nucleophiles in the active site of these enzymes and selecting appropriate reactive groups to provide covalent modification of the targeted enzymes (27, 28). For zinc metalloproteinases, like MMPs, the lack of conserved active-site nucleophiles requires the use of photolabile groups to covalently label the enzyme active site (23–26). Following this strategy, we recently developed a selective MMP probe that consists of a phosphinic peptide core able to block potently and selectively a large set of MMPs, to which an azido photolabile group has been grafted onto the inhibitor P₁' side chain (probe 1, Scheme 1) (26).

The choice of the photolabile group and position of its incorporation in the inhibitor structure were based on the x-ray structure of phosphinic peptide inhibitor in complex with MMP-9 (29). Based on these structural considerations, the

* This work was supported by funds from the Commissariat à l'Energie Atomique and from the European Commission (Grant FP6RDT, Cancer Degradome project, LSHC-CT-2003-503297). The costs of publication of this article were defrayed in part by the payment of page charges. This article must therefore be hereby marked "advertisement" in accordance with 18 U.S.C. Section 1734 solely to indicate this fact.

¹ To whom correspondence should be addressed: Tel.: 33-1-6908-2603; Fax: 33-1-6908-9071; E-mail: vincent.dive@cea.fr.

² The abbreviations used are: MMP, matrix metalloproteinase; hMMP-12, human matrix metalloelastase; Mca, (7-methoxycoumarin-4-yl)acetyl; Dpa, N³-(2,4-dinitrophenyl)-L-2,3-diaminopropionyl; Mca-Mat, Mca-Pro-Leu-Gly-Leu-Dpa-Ala-Arg-NH₂; FA, formic acid; ABP, activity-based probe; RP-HPLC, reversed-phase high-performance liquid chromatography; PVDF, polyvinylidene difluoride; ESI, electrospray ionization; MS, mass spectrometry; MS/MS, tandem MS.



SCHEME 1

azido group of probe **1** is expected to enter into the deep S_1' cavity of MMPs, in a position that should favor covalent modification of residues lining this cavity. While probe **1** was shown to covalently modify only the active site of MMPs, high variation in cross-linking yield was observed between different MMPs (26). Indeed, the covalent modification of hMMP-12 by probe **1** resulted in a cross-linking yield of $\approx 45\%$, whereas this yield decreased to a few percents for human MMP-8. To understand the molecular determinant of this difference and improve the design of better ABPs that covalently modified all MMPs with high cross-linking yields, the identification of the hMMP-12 residues covalently modified by probe **1** has been carried out.

EXPERIMENTAL PROCEDURES

Chemicals—Commercial reagents were used without additional purification. Buffers and salts were purchased from Sigma. Synthesis and tritium radiolabeling of probe **1** were carried out as previously reported (26). Mca-Pro-Leu-Gly-Leu-Dpa-Ala-Arg-NH₂ (Mca-Mat) was purchased from Novabiochem and TIMP-1 inhibitor from R&D Systems.

Proteins—Synthetic gene encoding the catalytic domain of the MMP-12 (Met⁹⁸–Lys²⁶⁶) was obtained from Geneart (Geneart-AG, Germany). This gene was inserted into the pET24a vector, between the NdeI and BamHI site, for expression under the PT7 promoter. A Lys \rightarrow Ala mutant was produced from 5'-ccgtaatgttcccacactacGCatagtgtgacatcaacaca-3' and 5'-tgtgtgtgatgcaacatGCGtaggtgggaacattacgg-3' oligonucleotides, using the Site-Directed Mutagenesis Kit (Stratagene). All plasmids were propagated in the *Escherichia coli* strain XL1-Blue at 37 °C, and all constructions were verified by DNA sequencing using the ABI PRISM 310 Genetic analyzer (Applied Biosystems). Recombinant proteins were expressed in *E. coli* BL21(DE3 star) cells carrying the MMP-12 catalytic domain-encoding plasmids. Bacteria were grown at 37 °C in LB medium supplemented with kanamycin (50 μ g/ml). At an absorbance (600 nm) of 0.6, protein expression was induced with 0.5 mM isopropyl- β -thiogalactopyranoside. Five hours

after induction, cells were harvested by centrifugation at $5000 \times g$ for 30 min at 4 °C. The pellets were resuspended in buffer A (100 mM Tris-HCl, pH 8.5, 5 mM benzamidinechloride, 5 mM 2-mercaptoethanol) and incubated with lysozyme for 1 h at 4 °C. The suspension was then passed through a cell disruption system at 4 °C (Constant Systems Ltd., Daventry Northants, England) and was then centrifuged at 4 °C for 30 min ($8000 \times g$). The pellets were washed three times with buffer B (100 mM Tris-HCl, pH 8.5, 2 M urea, 5 mM 2-mercaptoethanol) and dissolved in buffer C (100 mM Tris-HCl, pH 8.5, 8 M urea). Refolding and purification steps were carried out as previously described (30). Refolded proteins were analyzed by SDS-PAGE and found to migrate as a single band. Protein molecular weights were determined by electrospray ionization-mass spectrometry and the presence of the Lys \rightarrow Ala mutation was verified by matrix-assisted laser desorption ionization time-of-flight, after tryptic digestion.

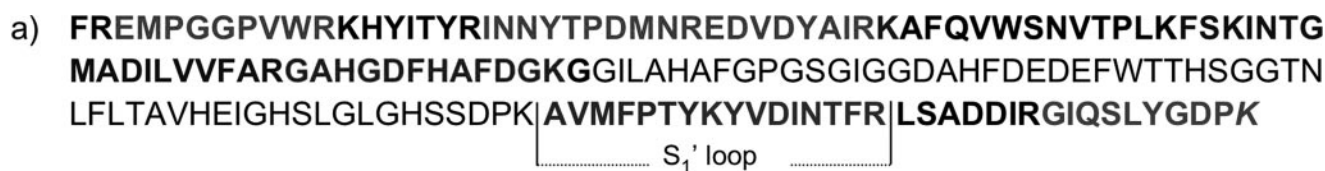
Enzyme Assays—Enzyme assays and inhibition and titration experiments were carried out in 50 mM Tris/HCl buffer, pH 6.8, 10 mM CaCl₂, at 25 °C, in flat-bottomed 96-well nonbinding surface plates (Corning-Costar, Schiphol-Rijk, The Netherlands), using the Mca-Pro-Leu-Gly-Leu-Dpa-Ala-Arg-NH₂ (Mca-Mat) substrate, as described before (15). Fluorescence signals were monitored using a Fluoroscan Ascent photon counter spectrophotometer (Thermo-Labsystems) equipped with a temperature control device and a plate shaker. Titration experiments using a calibrated TIMP-1 solution were performed to determine the exact enzyme concentration for each MMP batch: for these experiments, MMP concentrations were set at ~ 20 nM. Values for k_{cat}/K_m were determined from first-order full-time course reaction curves obtained at $[S] \ll K_m$ ($[S] = 0.5$ mM) and 5 nM final enzyme concentration. These progress curves were monitored by following the increase in fluorescence at 400 nm ($\lambda_{\text{ex}} = 340$ nm) induced by the cleavage of the Mca-Mat substrate. k_{cat}/K_m values were obtained by fitting these progress curves (three independent experiments) with the integrated Michaelis-Menten equation by nonlinear regression. The K_i values of probe **1** were determined using the method proposed by Horovitz and Leviski (31).

Mass Spectrometry—MS experiments were performed on an Ion Trap mass spectrometer (Bruker, Esquire-HCT). Ion trap parameters were set as follows: electrospray potential, ± 4000 V; skimmer voltage, ± 40 V; capillary exit, 226 V; and a source temperature of 365 °C. The MS survey scan was m/z 400–3000 Da with a target mass fixed at m/z 1800 Da and a 5-spectrum scan average.

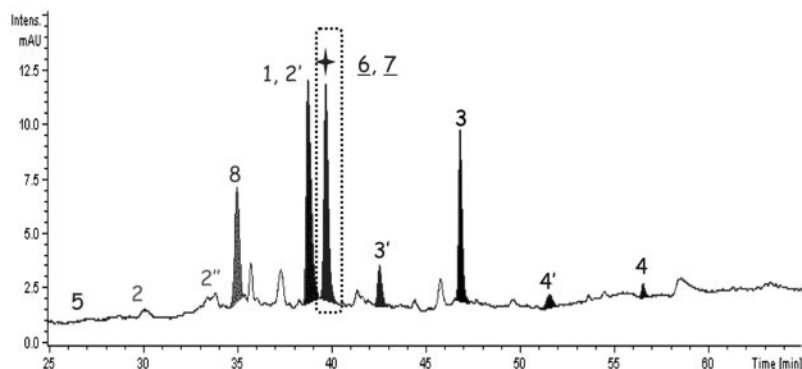
Nano-RP-HPLC—Peptide separation was carried out on an Ultimate LC Packings/DIONEX UltiMate™ Capillary/Nano-LC System apparatus, using an Acclaim PepMap100 C₁₈, 3 μ m, 100 Å (150 mm \times 75 μ m) column at a flow rate of 200 nL \cdot min⁻¹ and with detection at 214 nm. Solvent systems were: (A) 95% water, 5% acetonitrile, 0.01% trifluoroacetic acid, and 0.04% FA and (B) 5% water, 95% acetonitrile, 0.01% trifluoroacetic acid, and 0.04% FA. The following gradient was used: $t = 0$ min, 100% A; $t = 3$ min, 100% A; $t = 73$ min 70% B; $t = 74$ min 100% B; and $t = 80$ min 100% B.

μ -RP-HPLC—Peptide separation was carried out on an Agilent 1100 series apparatus and using a X-Bridge (Waters) C₁₈

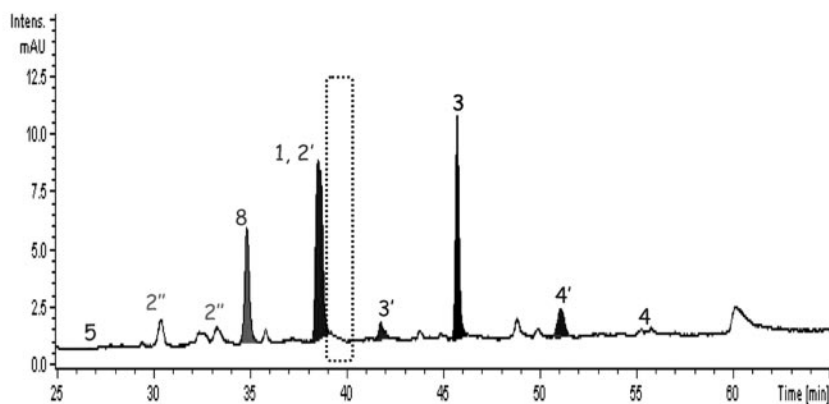
MMP-12 Photoaffinity Probe



b) (-) probe



c) (+) probe



d)

- 1: EMPGGVWR [MH]⁺ = 1028.7
- 2: INNYTPDMNR [MH]⁺ = 1237.7
- 2': EDVDYAIR [MH]⁺ = 980.6
- 2'': INNYTPDMNREDVDYAIR [MH]⁺ = 2200.0
- 3: AFQVWSNVTPLK [MH]⁺ = 1389.7
- 3': KAFQVWSNVTPLK [MH]⁺ = 1518.2
- 4: INTGMADILVVFAR [MH]⁺ = 1520.2
- 4': INTGM(Ox)ADILVVFAR [MH]⁺ = 1536.6
- 5: GAHGDHFHAFDGGK [MH]⁺ = 1258.8
- 6: AVMFPTYK [MH]⁺ = 956.6
- 7: YVDINTFR [MH]⁺ = 1027.7
- 8: GIQSLYGDPK [MH]⁺ = 1077.7

FIGURE 1. Peptide fragments generated by trypsin cleavage of hMMP-12. *a*, sequence showing the tryptic fragments of hMMP-12 catalytic domain. Nano-HPLC profile (214 nm) of a tryptic peptide mixture obtained by in-gel digestion of unmodified (*b*) or covalent (*c*) hMMP-12 by probe **1** (loading of 5 pmol). *d*, tryptic peptide sequences of hMMP-12 and corresponding *m/z* ratio. Numbers in *b* and *c* and their correspondence in peptide sequence are reported in *d*.

5- μ m, 300- Å column (2.1 \times 150 mm, 5 μ m) at a flow rate of 200 μ l/min and with detection at 214 nm. Solvent systems were: (A) 100% water, 0.1% FA and (B) 100% acetonitrile, 0.09% FA. The following gradient was used: $t = 0$ min, 10% B; $t = 5$ min, 10% B; and $t = 45$ min 100% B.

Photoaffinity Labeling—MMPs (1 μ M) were incubated with 2 μ M of ³H probe **1** in 50 mM Tris/HCl, pH 6.8, 10 mM CaCl₂, 0.01% Brij35, for 10 min in the dark at room temperature. The reaction mixture was irradiated using a 1000-watt mercury

lamp (Orsam) for 2 min (10 °C). All irradiation experiments were performed under inactinic light (sodium light) at 310 nm (50 microwatts \cdot cm⁻²) on an apparatus equipped with an aperture and a series of lenses focusing the polychromatic light to a monochromator (Jobin-Yvon), a series of lenses to focus the monochromatic light to a thermostat support, in which the Eppendorf tube containing the mixture to irradiate is inserted. Light intensity was measured with a radiometer IL1700 (International Light, Newburyport, MA). After irradiation, the reac-

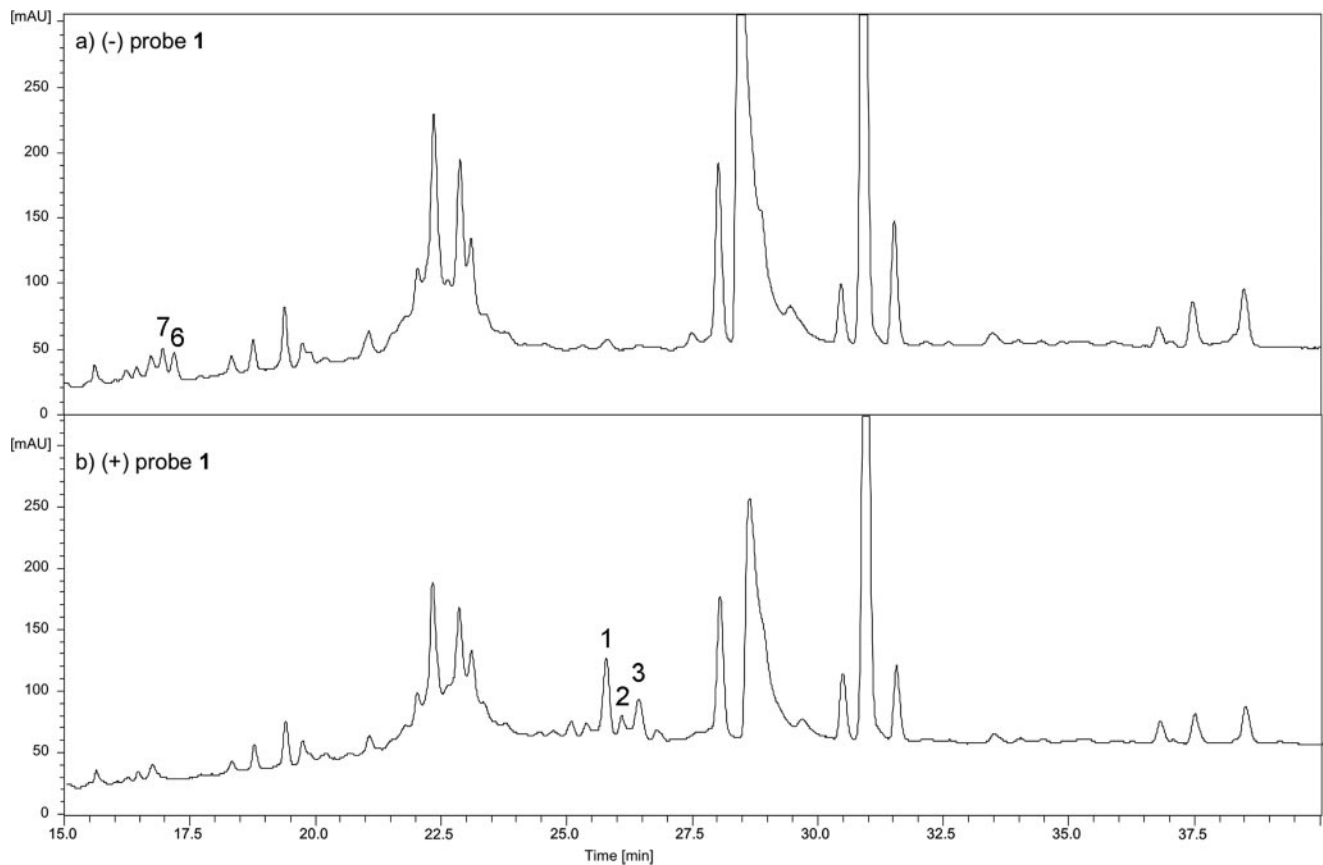


FIGURE 2. μ -HPLC profile of a tryptic peptide mixture obtained by trypsin digestion of unmodified or covalently modified hMMP-12 by probe 1. UV trace (214 nm) of PVDF tryptic digest (100 pmol) of unmodified (a) and modified (b) hMMP-12 by probe 1. In a peaks labeled 6 and 7 correspond to the two tryptic fragments reported in Fig. 1 generated by trypsin cleavage of the S_1' loop. In b peaks labeled 1, 2, and 3 correspond to tryptic fragments covalently modified by probe 1.

tion was quenched by the addition of Laemmli loading buffer followed by boiling (5 min, 95 °C). These samples were immediately processed for subsequent SDS gel analysis.

Electrophoresis—Radiolabeled proteins were diluted in Laemmli loading buffer (final concentration, 0.1% (w/v) bromophenol blue, 2% (w/v) SDS, 10% (v/v) glycerol, 50 mM Tris-HCl, pH 6.8, and 100 mM dithiothreitol) and were resolved by SDS-PAGE electrophoresis in a 12% 1 mm-thick SDS gel, using a mini-protean III apparatus (Bio-Rad). Silver staining was performed as classically described.

In-gel Digestion—Gels were stained with Coomassie Blue R250. Gel pieces containing proteins were excised and destained by adding 50 μ l of 25 mM NH_4HCO_3 in 50% acetonitrile. After a 10-min incubation with occasional vortexing, the liquid phase was discarded. This procedure was repeated three times. Gel pieces were then rinsed (10 min) with acetonitrile and dried under vacuum. Gel pieces were reswelled in 25 mM NH_4HCO_3 buffer containing trypsin (12 ng/ μ l, modified porcine trypsin sequence grade, Promega, Madison, WI). After the trypsin digestion (37 °C, 18 h), the solution was transferred into an Eppendorf tube, and tryptic peptides were isolated by extraction with 50 μ l of 50% acetonitrile in water with 1% FA (2 \times 10 min) at room temperature. Peptide extracts were pooled, concentrated under vacuum, and solubilized in 50% acetonitrile in water with 1% trifluoroacetic acid.

Blotting—Transfer of proteins onto a polyvinylidene fluoride (PVDF) membrane was achieved using a semi-dry transfer blot apparatus (Bio-Rad). Gels were rinsed in a 50 mM Tris/HCl, pH 8.5, 20% methanol, 40 mM glycine, 0.0375% SDS in distilled water (Transfer Buffer). The PVDF membrane was activated in a bath of methanol, rinsed with water, and then equilibrated in the transfer buffer. We formed a membrane sandwich for protein transfer between the cathode and the anode: this included, from anode to cathode, a sheet of extra thick blot paper (Bio-Rad), wetted with transfer buffer, then the activated PVDF membrane, the gel, and finally 2 sheets of extra thick blot paper wetted with transfer buffer. After transfer, membranes were dried before radioactivity analysis or were stained using a Coomassie Blue solution (0.1% R_{250} , 50/49/1 water/ethanol/acetic acid).

Radioimaging—Radioactivity imaging and counting of the PVDF membranes were performed with the beta-ImagerTM 2000 from Biospace (Paris, France). This apparatus allows an absolute counting of the tritium β particles, with a detection threshold of 0.007 cpm/ mm^2 for tritium.

Trypsin Digestion of PVDF Membranes—Pieces of PVDF membranes containing labeled or unlabeled hMMP-12 were excised and destained using a 50/50 water/ethanol solution to remove excess of R_{250} . PVDF pieces were incubated in a solution of 50 mM NH_4HCO_3 , pH 8/acetonitrile (50/50) with trypsin (12.5 ng/ μ l). Digestion was continued for 18–20 h at 50 °C.

MMP-12 Photoaffinity Probe

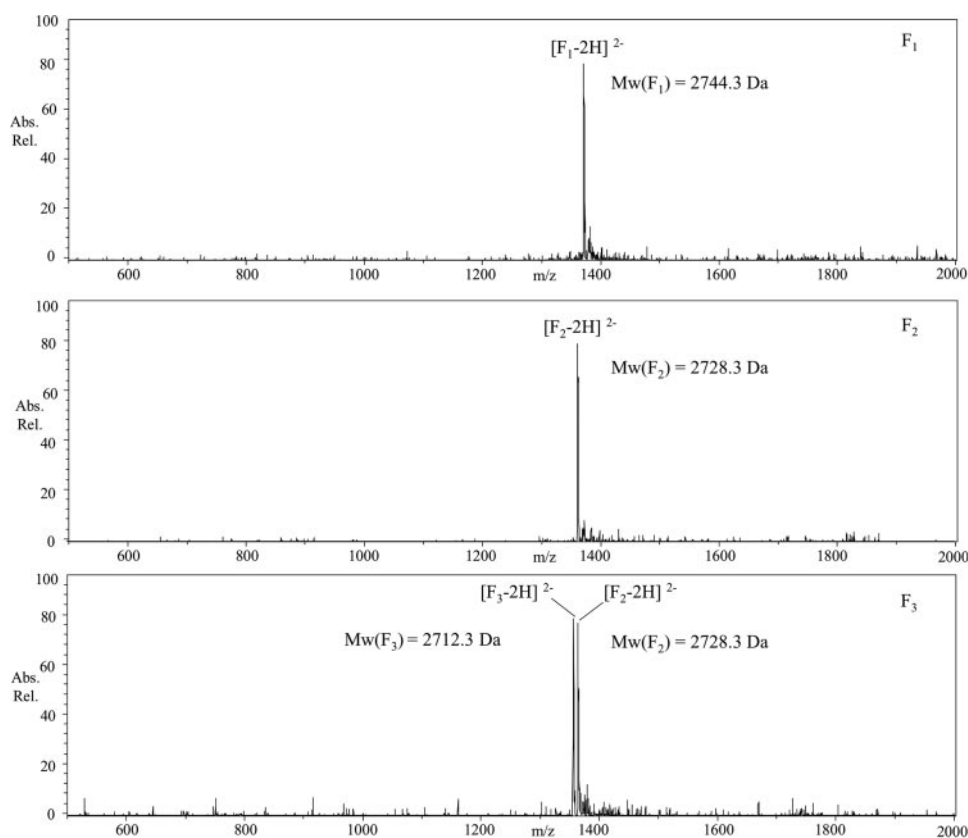


FIGURE 3. μ -HPLC ESI mass spectra (negative mode) of peaks 1, 2, and 3 reported in Fig. 2. Molecular weights corresponding to the double-charged ion species contained in these HPLC fractions are reported.

PVDF pieces were then rinsed with a solution of 50% acetonitrile with 0.1% trifluoroacetic acid.

Peptide Mapping—Eluant from the μ -HPLC column was split out into two flows: one at 160 μ l/min for UV monitoring (214 nm and 280 nm using a diode array detector) and radioactivity measurements; the remaining flow was directed to an electrospray mass spectrometer for MS. A volume of 0.5 μ l of each fraction was spotted onto a glass plate for counting tritium radioactivity using the beta-ImagerTM 2000. On-line μ -HPLC/ESI/MS experiments were performed on an ion trap mass spectrometer, with the parameters as described above.

Edman Sequencing—N-terminal amino acid sequence analysis was performed by automated Edman degradation using an ABI Model 477A/120A Protein-Peptide Sequencing/Analysis System and Analysis Software System, Model 920A (Applied Biosystems Inc., Foster City, CA). Radioactive fractions eluted from the μ -HPLC column were pooled and loaded onto a trifluoroacetic acid-treated cartridge filter, previously conditioned with BioBrene PlusTM. Prior to each sequence analysis, calibration was performed using a PTH-amino acid standard solution.

MS/MS Sequencing of Covalently Modified Peptides—Radioactive fractions containing covalent adduct peptides were concentrated by using a reverse phase pipette tip (C₁₈ ZipTip). Off-line nano-electrospray ionization-mass spectrometry/MS experiments were performed on a ion trap mass spectrometer. Ion trap parameters for MS were set as follows: nano-electrospray potential, 1000 V; skimmer voltage, 40 V; capillary exit, 226 V; and source temperature, 150 °C. The scan number was

increased to 20 spectra over an m/z of 250–2000 Da, the isolation width was set to 1 Da, and the collision energy to 0.65 V in the MS/MS-mode. MS/MS spectra were recorded for double-charged molecular peptide ions.

Molecular Modeling—Model of probe 1 interacting with hMMP-12 was obtained as previously described (15). NMR structures in Fig. 7 (a and b) were selected from an ensemble of 20 NMR structures of the hMMP-12 catalytic domain deposited in Rutgers Collaboratory for Structural Bioinformatics PDB under access code 2POJ.

RESULTS

One-dimensional SDS-PAGE In-gel Digestion—Efficient cross-linking experiments were shown to rely on the presence of detergent in sample buffer, a requirement preventing direct analysis of the photo-adduct by MS. In addition, previous work has demonstrated that light excitation of probe 1 in the presence of hMMP-12 catalytic domain produced two protein species that

could be resolved by one-dimensional SDS-PAGE, the upper band corresponding to the covalently labeled hMMP-12 and the lower band to unmodified hMMP-12 (26). These considerations led us to use first electrophoresis to separate the unmodified from modified forms of hMMP-12 and then proceed to the analytical characterization of these protein species. After electrophoresis, gel pieces containing these protein forms were subjected to in-gel trypsin digestion, and the corresponding soluble tryptic fragments were resolved by nano-HPLC and analyzed online by MS. Nano-HPLC-MS analyses of the tryptic fragments from unlabeled (Fig. 1b) hMMP-12 showed a good overlapping with its catalytic domain sequence (Fig. 1a). Among the 12 expected tryptic fragments, 8 fragments were detected in the nano-HPLC profile (Fig. 1, b and d). Based on mass criteria, two peptides co-eluting at the same retention time were shown to result from the S₁' loop cleavage by trypsin (peak 6: MH⁺ = 956.6 and 7: MH⁺ = 1027.5; through this report, the S₁' loop sequence corresponds to the fragment Ala²³⁴ to Arg²⁴⁹). The nano-HPLC profile (Fig. 1c) for the covalently modified form of hMMP-12 (*upper band*) was characterized by an absence of peaks 6 and 7. This suggests that the covalent modification of hMMP-12 by the probe targets residues of the S₁' loop. No additional signals corresponding to modified peptides were observed in this nano-HPLC profile, thus the corresponding peptides should remain in the gel. An absence of radioactivity in the sample buffer (probe 1 incorporates a tritium radioactive atom, Scheme 1) supports this con-

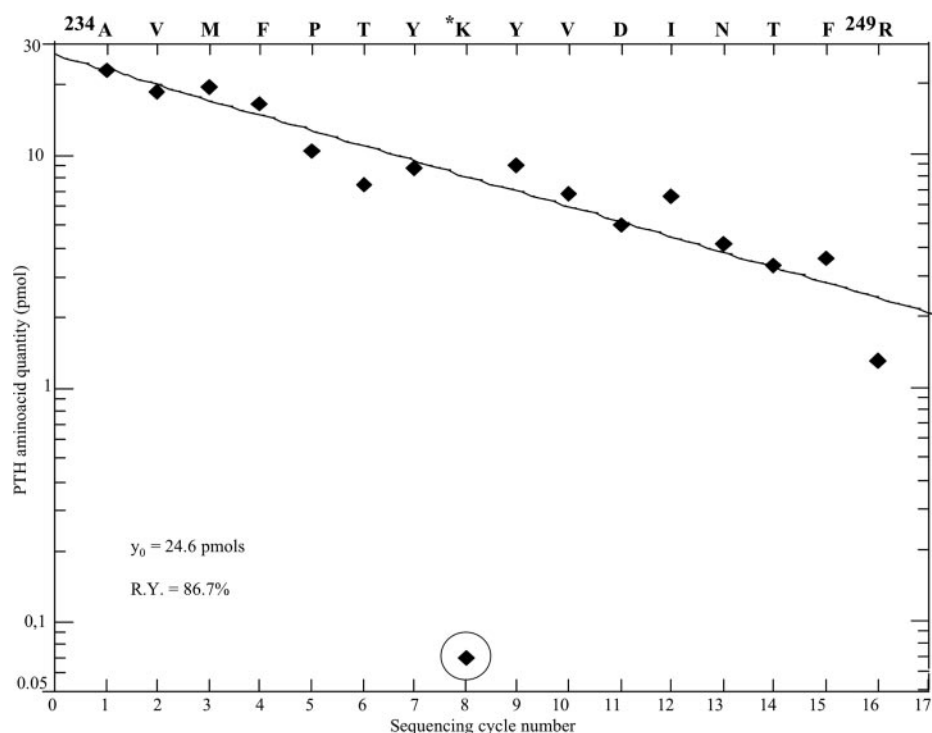


FIGURE 4. Edman degradation of the purified fragment peptide of hMMP-12 (25 pmol) covalently modified by probe 1.

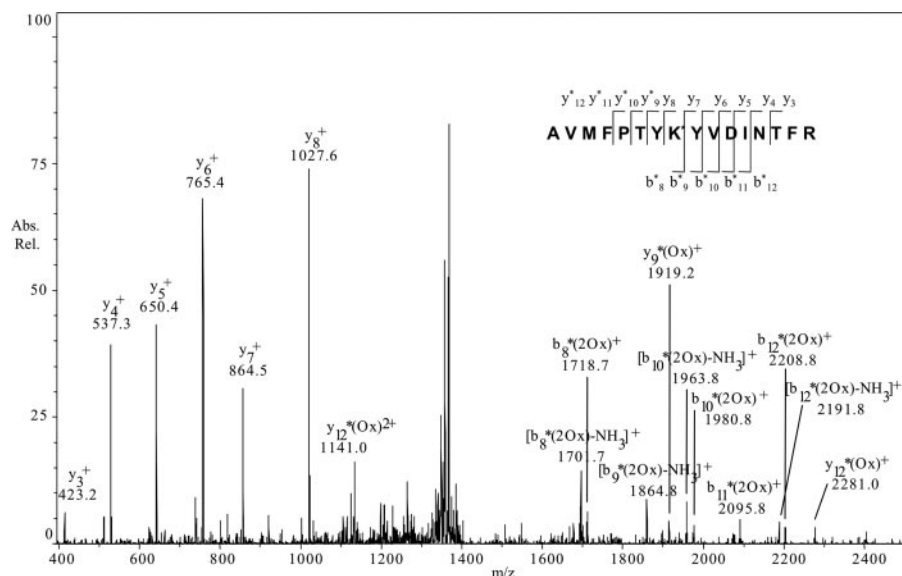


FIGURE 5. Low energy collision induced dissociation spectrum of the purified S_1' loop peptide fragment modified by probe 1, precursor ion at m/z 1373.1 (double-protonated ion with two degrees of oxidation). The mass shift observed for the y_9 ion, corresponding exactly to the mass increment expected for the covalent addition of probe 1 to the S_1' loop fragment, including one degree of oxidation, demonstrated that the covalent modification occurs at Lys²⁴¹ level.

clusion. To overcome this drawback, proteins were transferred from the gel onto PVDF membranes, prior to trypsin treatment.

Micro Liquid Chromatography-MS Analysis of Tryptic Digest Containing Radioactive Species—Analysis of PVDF membranes after gel transfer by radioimaging indicated a quantitative protein transfer. When pieces of PVDF membrane containing hMMP-12 covalently labeled by probe 1 were incubated in buffer, no signal of radioactivity was detected in solution, a result showing that labeled hMMP-12 remains on/in the mem-

brane. By contrast, when these membranes were incubated in buffer containing trypsin, radioactivity was released, suggesting the presence of hMMP-12 tryptic fragment(s) labeled by probe 1 in buffer sample. This tryptic fragment mixture, including those obtained from unmodified hMMP-12, were analyzed by μ -HPLC, MS, and radioactivity counting. Comparison of the corresponding μ -HPLC profiles (Fig. 2a unlabeled hMMP-12 and 2b labeled hMMP-12) revealed the presence of three additional radioactive peaks in the labeled sample. S_1' loop tryptic fragments (peaks 6 and 7 in Fig. 2a) were detected in the unlabeled hMMP-12 sample, but were no longer detected in the labeled sample, suggesting again a covalent modification of the S_1' loop by the photoaffinity probe.

MS Analysis of the Three Radioactive Peptides—Measure of mass-to-charge ratio using a negative detection mode of the above three μ -HPLC peaks (F1, F2, and F3) indicated that the mass of the fragment contained in F3 corresponds approximately to the expected mass (observed mass 2712.3 Da, expected mass 2713.3 Da, see "Discussion") of the S_1' loop peptide of hMMP-12 (residues Ala²³⁴ to Arg²⁴⁹, M_w = 1964.99) covalently modified by probe 1 (M_w = 776.27 Da, minus 28 Da due to loss of N_2 after irradiation of the azide group) (Fig. 3). Thus, the covalent modification of hMMP-12 by probe 1 prevents cleavage of the S_1' loop peptide by trypsin, a result explaining why the corresponding tryptic fragments are no longer detected after covalent modification. Furthermore, this absence of trypsin cleavage suggests that the site of covalent modification occurs at the Lys²⁴¹ level or at a residue near Lys²⁴¹ (the S_1' loop fragment contains only one internal tryptic site). The mass-to-charge ratio of the two other species (F1 and F2 in Fig. 3) corresponds to F3-oxidized forms, with one (+16, F2) and two (+32, F1) degrees of oxidation, respectively. The presence of Met²³⁶ in the S_1' loop sequence may explain the observation of oxidized forms (see below).

Edman Sequencing—The three purified radioactive fractions (F1, F2, and F3), containing the covalently modified hMMP-12 S_1' loop peptide, were pooled and subjected to Edman degra-

MMP-12 Photoaffinity Probe

dation to further characterize the site of covalent modification. N-terminal sequencing of this peptide started at Ala²³⁴ and ended at to Tyr²⁴⁰, with no sequencing cycle detected at the Lys²⁴¹ position (Fig. 4). The next sequencing step indicated a Tyr residue at position 242, and sequencing identified all subsequent S₁' loop residues up to Arg²⁴⁹. Therefore, the site of covalent modification occurs in the S₁' loop, and Lys²⁴¹ is the only residue modified by probe **1** in this loop.

MS/MS Analysis—The MS/MS analysis of the purified and photo-cross-linked tryptic fragments corresponding to the S₁' loop was carried out for further confirmation and to characterize the chemical structure of the covalent adduct. MS/MS (collision induced dissociation) experiments were performed on the double-charged precursor ion at $m/z [M+2H]^{2+} = 1373.1$ Da, corresponding to the double oxidized modified tryptic peptide (Mw(F1) = 2744,3 Da, Fig. 3). Fragment ions were assigned according to the nomenclature described by Biemann *et al.* (32). Experimental C-terminal γ_3 to γ_8 ion masses were consistent with those predicted, indicating that the C-terminal part of the S₁' loop from Tyr²⁴² to Arg²⁴⁹ is not modified by probe **1** (Fig. 5). All these ions possess the expected theoretical mass, thus no oxidation takes place in the Tyr²⁴²–Arg²⁴⁹ sequence. By contrast, the mass shift observed from ion γ_9 to γ_{12} , corresponding exactly to the mass increment expected for the covalent addition of probe **1** to the S₁' loop fragment, including one degree of oxidation, demonstrated that the covalent modification occurs at the Lys²⁴¹ level. Because this part of the S₁' loop does not contain a methionine or amino acids that could be the target of oxidation (Pro²³⁹–Arg²⁴⁹), the oxidation site in this case is expected to occur inside the probe structure. Observed N-terminal b ion masses (from b₈ to b₁₂) are in agreement with the above conclusion, but these observations alone cannot be

used to determine the site of modification. This identification would have required observing the b₇ ion, at the least. All b ions observed possess two degrees of oxidation, one as a result from probe oxidation, as suggested above, and the other probably resulting from methionine oxidation.

Analysis of Lysine → Ala Mutant—An hMMP-12 mutant was produced in which lysine in position 241 of the wild type was replaced by alanine. Comparison of the catalytic efficiency of this mutant in cleaving a fluorogenic synthetic substrate specific for MMPs, as well as the K_i value of probe **1** toward the mutant, as compared with wild-type hMMP-12, indicates similar functional properties between the two proteins (Table 1). Photolabeling of this mutant with probe **1**, analyzed either by silver staining or radioactivity counting, revealed significantly less cross-linking in the mutant ($\approx 2\%$ based on radioactivity counting), than in wild-type hMMP-12 ($\approx 45\%$) (Fig. 6).

DISCUSSION

The various approaches used in this study indicate that modification of hMMP-12 by probe **1** mostly involved the ϵ amino group of Lys²⁴¹, a residue located on the S₁' loop, shaping one part of the S₁' cavity (26). This is consistent with our previous suggestions that grafting an azide onto a P₁' phenylisoxazoline side chain of a phosphinic peptide inhibitor of MMP should result in a photoaffinity probe able to modify residues of the S₁' cavity. However, even by using a molecular model describing the potential binding mode of **1** within the hMMP-12 active site, it would be hard to predict the results reported in this study. The main reason for this is the fact that Lys²⁴¹ is located on a loop segment of hMMP-12, which, based on both x-ray and NMR studies of free hMMP-12 or in complex with synthetic inhibitors, displays high flexibility with the lysine side chain exhibiting high mobility (33–35). Superimposition of two hMMP-12 structure models, taken from an ensemble of twenty NMR-derived free hMMP-12 structures (34), provides some clues about the conformational space sampled by the Lys²⁴¹ side chain (Fig. 7). In one of these structures, the position taken by the ϵ amino group of Lys²⁴¹ is too far away ($d > 7 \text{ \AA}$) from the presumed position of the nitrogen atom of the reactive intermediate to predict covalent labeling of the lysine side chain (Fig.

7a). By contrast, the second structure, in which the ϵ amino group of Lys²⁴¹ points toward the S₁' loop cavity, would favor the labeling of Lys²⁴¹ by probe **1** (Fig. 7b). It is worth noting that, in these NMR structures, the positions reported for the lysine side chain correspond only to “possible conformations.” Result of the photo-cross-link experiments thus leads credence to these models, in particular to the one in which the lysine side chain points toward the S₁' cavity. The binding of probe **1** to hMMP-12 may induce a conformational change and stabilize a structure similar to that reported in Fig. 7b, in

TABLE 1
Characterization of hMMP-12 Ala mutant

k_{cat}/K_m and K_i values were determined in Tris/HCl buffer, 50 mM, pH 6.8, CaCl₂, 10 mM.

	hMMP-12	Ala mutant
Mca-Mat (k_{cat}/K_m , M ⁻¹ ·s ⁻¹)	1.53.10 ⁴ ($\pm 0.03.10^4$)	1.32.10 ⁴ ($\pm 0.05.10^4$)
Probe 1 (K_i , nM)	0.17 (± 0.01)	0.35 (± 0.04)

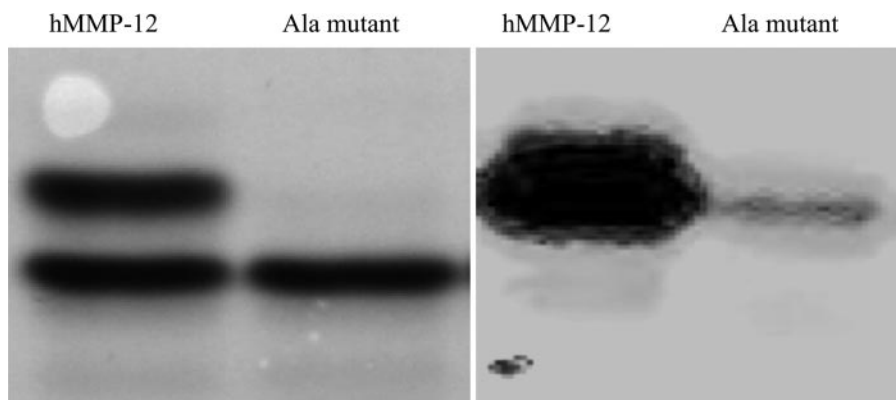


FIGURE 6. Comparison of the covalent modification of wild-type hMMP-12 and Ala mutant by probe 1. hMMP12 (1 μM) was incubated with probe **1** (2 μM) for 10 min, before UV irradiation (2 min). The MMP12 complexes (5 pmol) were resolved by one-dimensional SDS-PAGE electrophoresis and visualized on the gel by silver staining (left) or the proteins were transferred onto a PVDF membrane that was analyzed with a radioimager (right).

which the ϵ amino group of Lys²⁴¹ is pointing in the direction of and is in close proximity of the probe **1** azide group. Alternatively, movements of the lysine side chain may exist on a time scale faster than the lifetime of the nitrene reactive intermediate. The mass observed for the covalently modified S₁' loop corresponds to the theoretical expected mass minus 1. This difference was resolved by considering that the ϵ amino group of Lys²⁴¹ is actually labeled in its unprotonated form (NH₂). The equilibrium between NH₃⁺ and NH₂ forms at pH 7 of the Lys ϵ

amino group could be shifted toward the NH₂ form, through consumption of the NH₂ form by the photochemical reaction. Alternatively, a shift in the lysine conformation toward the nitrene reactive group may change the pK_a of that side chain. The exact chemical structure of the covalent adduct formed between hMMP-12 and probe **1**, after irradiation, has not been established in this study. Based on previous studies of aryl azides, irradiation of probe **1** is expected to produce as reactive intermediates either a dedihydroazepine (Scheme 2a) or a triplet nitrene (Scheme 2b), as reactive intermediates (36–38). The dedihydroazepine intermediate is thought to react with nucleophilic atoms present in cysteine and histidine residues, but less likely with the protonated ϵ amino group of the lysine side chain (Scheme 2, adduct **2a**) (38). Triplet nitrene may covalently modify the ϵ amino group of a lysine to form the structure reported in Scheme 2 (adduct **2b**). Simple phenylazides produce dedihydroazepine upon photolysis in water or buffer (39). However, the photogenerated intermediate was also reliant on the nature of the substituents of the phenyl ring (36–38). How the isoxazoline group in para-position

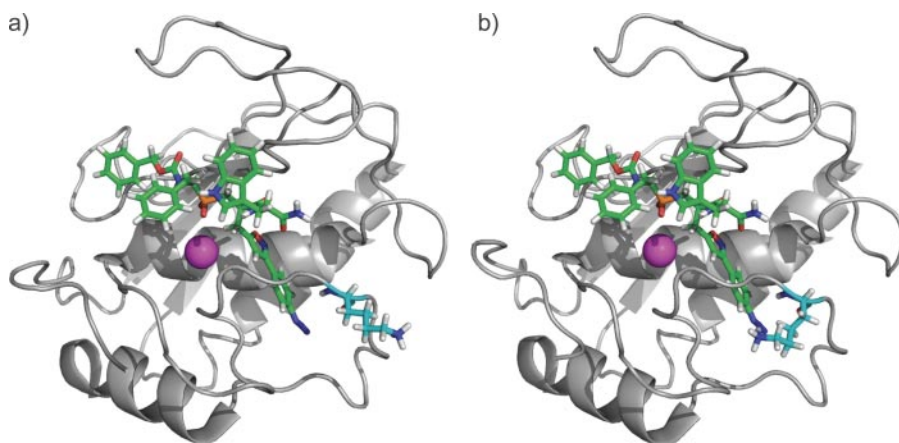
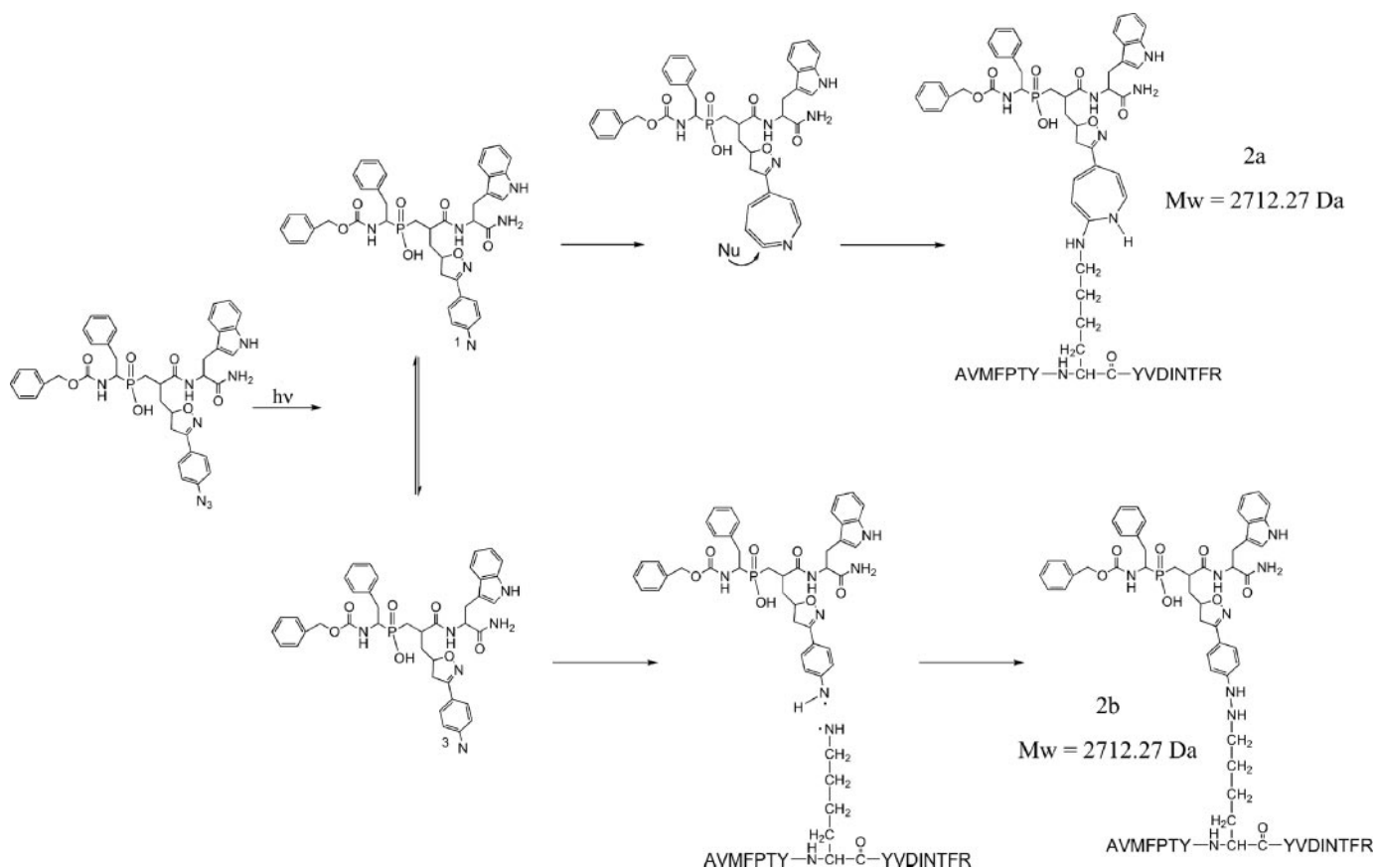


FIGURE 7. Model of probe **1** in complex with hMMP-12 (see “Experimental Procedures”). As compared with the standard orientation recommended for metzincins, the structure of MMP-12 catalytic domain has been tilted around the *horizontal axis* to better bring out the S₁' loop. Lys²⁴¹ is colored in blue, probe **1** in green, and catalytic zinc ion in purple; *a* and *b* displayed two possible conformations taken by the Lys²⁴¹ flexible side chain, one (*a*) far away from the azide group and the other (*b*) nearby this group.



SCHEME 2

MMP-12 Photoaffinity Probe

of the phenyl in probe **1** influences which type of reactive intermediate is formed is actually unknown. Moreover, in a context of high affinity, the protein binding site environment might determine the structure of the reactive intermediate that will be formed upon photolysis. Because the two predicted adducts have the same mass (Scheme 2, **2a** and **2b**), their discrimination by MS and the identification of the reactive intermediate involved in the reaction cannot be achieved in the present study. Indeed, given the length of adducts **2a** and **2b**, ESI/MS/MS mostly leads to peptide bond fragmentation. Thus, characterization of N–C or N–N bonds to discriminate between **2a** and **2b** adducts would require the use of other techniques like electronic impact. The few percent of covalent modification observed in the Ala mutant prevented further characterization of the covalent modification site. Similar weak covalent modifications occurring in the Ala mutant may also take place in wild-type hMMP-12, but this should only be considered as a minor reaction, in comparison with the major modification observed at lysine. Inspection of the S_1' cavity of hMMP-12 in the vicinity of the azide of probe **1** indicated that the closest atoms to the nitrogen linked to the phenyl (the one that will form the nitrene) are the $H\alpha$ ($d \approx 3\text{\AA}$) and $CH_3\gamma$ ($d \approx 3.5\text{\AA}$) of Val²³⁵. Labeling of hydrophobic residues is generally observed with probes that generate extremely reactive species like carbene (38), thus the weak labeling observed in the Ala mutant may be explained by the weaker reactivity of the nitrene formed by probe **1** toward hydrophobic residues, like Val²³⁵. Interestingly, in MMP-8 in which the position 241 is occupied by an alanine, a weak labeling (~2–3%) was previously reported for its covalent modification by probe **1** (26). Thus, MMP-8 and the Ala-MMP-12 mutant display a similar reactivity toward probe **1**, even though their S_1' loop sequences are very different. Thus cross-linking yield between probe **1** and other MMPs is possibly determined by the chemical nature of the residue in position 241. This may explain the marked differences in cross-linking yield observed between various MMPs, because the composition of the position 241 is highly variable in MMPs (Ala_(MMP8), Gln_(MMP14), Thr_(MMP2, 13, 11), Arg_(MMP9), and His_(MMP3)). If true, developing photoaffinity probes with high cross-linking dedicated to MMPs (23–26), these ABP yield toward all MMPs will require the selection of other reactive photo-activable groups, having lower selectivity toward the chemical nature of the residues surrounding the probe. This challenge will have to overcome the various chemical constraints and the particular shape of the MMP S_1' cavity. Probing the S_1' cavity of MMPs by photoaffinity labeling, as shown here, provides a unique insight into the conformational variability of MMPs, a key factor governing their selective recognition of substrates or inhibitors. Despite the development of very smart and different activity-based probes (ABPs) probes have not yet detected active forms of MMPs in biological samples. The tight regulation and control of MMP active forms probably explain this failure, but it also calls for the development of extremely sensitive ABP probes (40). To be achieved, this goal needs to take into account the yield of cross-link achieved by these probes toward all MMP members. The data reported in this study should help in the design of better MMP ABP probes, allowing the sensitive detection of their active forms in various

samples, an important objective for both diagnosis and therapeutic application (41–43).

REFERENCES

1. Brinckerhoff, C. E., and Matrisian, L. M. (2002) *Nat. Rev. Mol. Cell. Biol.* **3**, 207–214
2. Visse, R., and Nagase, H. (2003) *Circ. Res.* **92**, 827–839
3. Page-McCaw, A., Ewald, A. J., and Werb, Z. (2007) *Nat. Rev. Mol. Cell. Biol.* **8**, 221–233
4. Nagase, H., and Woessner, J. F., Jr. (1999) *J. Biol. Chem.* **274**, 21491–21494
5. Bode, W., Gomis-Ruth, F. X., and Stockler, W. (1993) *FEBS Lett.* **331**, 134–140
6. Stocker, W., and Bode, W. (1995) *Curr. Opin. Struct. Biol.* **5**, 383–390
7. Massova, I., Lakshmi, P. K., Fridman, R., and Mobashery, S. (1998) *FASEB J.* **12**, 1075–1095
8. Gomis-Ruth, F. X. (2003) *Mol. Biotechnol.* **24**, 157–202
9. Fingleton, B. (2007) *Curr. Pharm. Des.* **13**, 333–346
10. Babine, R. E., and Bender, S. L. (1997) *Chem. Rev.* **97**, 1359–1472
11. Whittaker, M., Floyd, C. D., Brown, P., and Gearing, A. J. (1999) *Chem. Rev.* **99**, 2735–2776
12. Rosenblum, G., Meroueh, S. O., Kleinfeld, O., Brown, S., Singson, S., Fridman, R., Mobashery, S., and Sagi, I. (2003) *J. Biol. Chem.* **278**, 27009–27015
13. Engel, C. K., Pirard, B., Schimanski, S., Kirsch, R., Habermann, J., Kingler, O., Schlotte, V., Weithmann, K. U., and Wendt, K. U. (2005) *Chem. Biol.* **12**, 181–189
14. Johnson, A. R., Pavlovsky, A. G., Ortwine, D. F., Prior, F., Man, C. F., Bornemeier, D. A., Banotai, C. A., Mueller, W. T., McConnell, P., Yan, C., Baragi, V., Lesch, C., Roark, W. H., Wilson, M., Datta, K., Guzman, R., Han, H. K., and Dyer, R. D. (2007) *J. Biol. Chem.* **282**, 27781–27791
15. Devel, L., Rogakos, V., David, A., Makaritis, A., Beau, F., Cuniassse, P., Yiotakis, A., and Dive, V. (2006) *J. Biol. Chem.* **281**, 11152–11160
16. Coussens, L. M., Fingleton, B., and Matrisian, L. M. (2002) *Science* **295**, 2387–2392
17. Lopez-Otin, C., and Matrisian, L. M. (2007) *Nat. Rev. Cancer* **7**, 800–808
18. Overall, C. M., and Lopez-Otin, C. (2002) *Nat. Rev. Cancer* **2**, 657–672
19. Egeblad, M., and Werb, Z. (2002) *Nat. Rev. Cancer* **2**, 161–174
20. Overall, C. M., and Kleinfeld, O. (2006) *Nat. Rev. Cancer* **6**, 227–239
21. Fingleton, B. (2006) *Front. Biosci.* **11**, 479–491
22. Johnson, J. L., George, S. J., Newby, A. C., and Jackson, C. L. (2005) *Proc. Natl. Acad. Sci. U. S. A.* **102**, 15575–15580
23. Saghatelian, A., Jessani, N., Joseph, A., Humphrey, M., and Cravatt, B. F. (2004) *Proc. Natl. Acad. Sci. U. S. A.* **101**, 10000–10005
24. Chan, E. W., Chattopadhyaya, S., Panicker, R. C., Huang, X., and Yao, S. Q. (2004) *J. Am. Chem. Soc.* **126**, 14435–14446
25. Sieber, S. A., Niessen, S., Hoover, H. S., and Cravatt, B. F. (2006) *Nat. Chem. Biol.* **2**, 274–281
26. David, A., Steer, D., Bregant, S., Devel, L., Makaritis, A., Beau, F., Yiotakis, A., and Dive, V. (2007) *Angew. Chem. Int. Ed. Engl.* **46**, 3275–3277
27. Cravatt, B. F., Wright, A. T., and Kozarich, J. W. (2008) *Annu. Rev. Biochem.* **77**, 383–414
28. Kato, D., Boatright, K. M., Berger, A. B., Nazif, T., Blum, G., Ryan, C., Chehade, K. A., Salvesen, G. S., and Bogoy, M. (2005) *Nat. Chem. Biol.* **1**, 33–38
29. Tochowicz, A., Maskos, K., Huber, R., Oltenfreiter, R., Dive, V., Yiotakis, A., Zanda, M., Bode, W., and Goettig, P. (2007) *J. Mol. Biol.* **371**, 989–1006
30. Lang, R., Kocourek, A., Braun, M., Tschesche, H., Huber, R., Bode, W., and Maskos, K. (2001) *J. Mol. Biol.* **312**, 731–742
31. Horovitz, A., and Levitzki, A. (1987) *Proc. Natl. Acad. Sci. U. S. A.* **84**, 6654–6658
32. Biemann, K. (1990) *Methods Enzymol.* **193**, 886–887
33. Nar, H., Werle, K., Bauer, M. M., Dollinger, H., and Jung, B. (2001) *J. Mol. Biol.* **312**, 743–751
34. Bhaskaran, R., Palmier, M. O., Bagegni, N. A., Liang, X., and Van Doren, S. T. (2007) *J. Mol. Biol.* **374**, 1333–1344
35. Bertini, I., Calderone, V., Cosenza, M., Fragai, M., Lee, Y. M., Luchinat, C., Mangani, S., Terni, B., and Turano, P. (2005) *Proc. Natl. Acad. Sci. U. S. A.* **102**, 5334–5339

36. Bayley, H., and Staros, J. V. (1984) in *Azides and Nitrenes*, (E. F. V. Scriven, ed) pp. 433–490, Academic Press, New York
37. Fleming, S. A. (1995) *Tetrahedron* **51**, 12479–12520
38. Kotzyba-Hibert, F., and Goeldner, M. (1995) *Angew Chem. Int. Ed. Engl.* **34**, 1296–1312
39. Rizk, M. S., Shi, X., and Platz, M. S. (2005) *Biochemistry* **45**, 543–551
40. Heseck, D., Toth, M., Meroueh, S. O., Brown, S., Zhao, H., Sakr, W., Fridman, R., and Mobashery, S. (2006) *Chem. Biol.* **13**, 379–386
41. Unsal, D., Akyurek, N., Uner, A., Erpolat, O. P., Han, U., Akmansu, M., Mentis, B. B., and Dursun, A. (2008) *Am. J. Clin. Oncol.* **31**, 55–63
42. Kramer, F., Sandner, P., Klein, M., and Krahn, T. (2008) *Biomarkers* **13**, 270–281
43. Rydlova, M., Holubec, L., Jr., Ludvikova, M., Jr., Kalfert, D., Franekova, J., Povysil, C., and Ludvikova, M. (2008) *Anticancer Res.* **28**, 1389–1397